Researchers Journal of Science and Technology (REJOST)

Solar-Powered LED Phototherapy for Neonatal Jaundice in Rural Settings: Design, Fabrication, and Implications for Neonatal Care

Alpha Henry[1], Ibeachu P. Chinagorom[2], Debekeme William Bulubellemowei[3], Fiberesima Tamunokuro Ogboye[4]

Abstract

The study covered the design and fabrication of a solar powered light emitting diode (LED) phototherapy light for rural neonatal care. The aim of the study was to design and fabricate a solar based phototherapy unit with an interruptible power supply. The authors used both active and passive components to design the electronic circuit (PIC microcontroller, relays, 12V batteries, 100W solar panel, LEDs, transistors, IR transmitter and receiver, resistors, capacitors, jumper wires, LCD display and buzzer etc.) and metal sheets for fabrication of the casing. The design was tested and results showed that the phototherapy device was able to stay ON for about 12 hours continuously powering the phototherapy lights. The temperature monitoring and alarm system worked perfectly sounding the alarm above 38.5°C. The device was able measure bilirubin level at three categories namely normal, positive/ High and positive / Low through the Green, Red and Blue LEDs indicators and finally, for cost effectiveness the system cost ₦450,000 while other phototherapy device with bilirubin meter cost about ₦1,200,000. The study demonstrated the efficacy of the solar-powered LED phototherapy light for rural neonatal care, suggesting its implementation to enhance healthcare accessibility in underserved areas, potentially through partnerships with local healthcare providers or NGOs for widespread adoption.

✉ Alpha Henry: alpha.henry@example.com

[1] Department of Biomedical Technology, School of Science Laboratory Technology, University of Port Harcourt, Rivers State, Nigeria

[2] Department of Anatomy, University of Port Harcourt, Rivers State, Nigeria

[3] Department of Electrical Engineering, School of Engineering Technology, University of Port Harcourt, Rivers State, Nigeria

[4] Research and Development Department, Tryllion Business Network

Keywords: Phototherapy; Neonatal care; Jaundice; Solar-powered device; Bilirubin meter; Rural healthcare

Article history
Received: July 9, 2025
Received in revised form: August 31, 2025
Accepted for publication: September 4, 2025
Available online: September 12, 2025

1.0 Introduction

Neonatal jaundice, characterized by the accumulation of bilirubin in the blood, is a prevalent condition affecting approximately 60% of term infants and up to 80% of preterm infants within the first week of life (Muchowski, 2014). This condition arises primarily due to the immature hepatic conjugation process in newborns, leading to elevated levels of unconjugated bilirubin, which manifests as yellowing of the skin and sclera (Mitra & Rennie, 2017). Globally, an estimated 13 million infants are affected annually, with 9 million residing in developing countries where access to effective treatment is limited (Bhutani *et al*., 2013). If untreated, severe hyperbilirubinemia can progress to acute bilirubin encephalopathy or kernicterus, conditions associated with neurological damage and mortality, contributing to 5–14% of neonatal deaths in regions such as Nigeria (Diala et al., 2018). Phototherapy, a non-invasive treatment that uses light to convert bilirubin into water-soluble photoproducts for excretion, remains the standard of care due to its efficacy, safety, and simplicity (Maisels & McDonagh, 2008).

The mechanism of phototherapy involves the use of light in the 400–520 nm wavelength range, with peak efficacy at 460 nm, to facilitate the photoisomerization of bilirubin into lumirubin and other excretable forms (Ennever, 1990). Light-emitting diode (LED) phototherapy has gained prominence over traditional fluorescent or halogen-based systems due to its high-intensity, narrow-spectrum light (450–470 nm), low energy consumption, minimal heat production, and long lifespan of up to 20,000 hours (Vreman *et al*., 1998). Clinical studies have demonstrated that LED phototherapy reduces treatment duration compared to halogen sources (Martins *et al*., 2007) and offers comparable efficacy to compact fluorescent lamps while requiring less maintenance (Kumar et al., 2010). Additionally, LEDs produce less heat, reducing the risk of hyperthermia in neonates, particularly preterm infants who are prone to temperature instability (Aydemir *et al*., 2014).

Despite its effectiveness, the delivery of phototherapy in rural and resource-limited settings faces significant challenges. Unreliable electricity supply is a major barrier, as many rural healthcare facilities lack consistent power, disrupting continuous phototherapy, which is critical to prevent rebound hyperbilirubinemia (Chang *et al*., 2017). Conventional phototherapy units, which often rely on fluorescent or halogen lamps, are energy-intensive and costly, with procurement prices ranging from $5,000 to $10,000, making them inaccessible to low-resource settings (Abioye & Abiodun, 2019). The high operational costs, including maintenance and replacement of lamps, further exacerbate financial burdens on healthcare systems in developing countries (Seidman *et al*., 2003). Moreover, the reliance on non-renewable energy sources for these devices contributes to carbon emissions, raising environmental concerns and complicating sustainable healthcare delivery (Kalogirou, 2022).

Alternative approaches, such as filtered sunlight phototherapy, have been explored in resource-limited settings due to their low cost and accessibility (Slusher *et al*., 2014). However, filtered sunlight carries risks of ultraviolet (UV) and infrared exposure, which can cause skin damage or overheating, making it less safe for neonatal use (Vreman *et al*., 2004). Fiberoptic

phototherapy devices, while safer and portable, often deliver lower irradiance, requiring longer treatment durations (Yurdakök, 2015). Existing solar-powered phototherapy systems have shown promise in addressing power reliability issues, but many are not optimized for rural neonatal care. Common limitations include the lack of integrated monitoring systems for temperature and bilirubin levels, limited portability, and high production costs, which hinder widespread adoption (Abioye & Abiodun, 2019).

The global burden of neonatal jaundice underscores the need for innovative solutions tailored to resource-constrained environments. In sub-Saharan Africa, where neonatal mortality rates are among the highest, the incidence of severe jaundice is exacerbated by delayed diagnosis, limited access to healthcare facilities, and inadequate treatment infrastructure (Olusanya *et al*., 2014). The World Health Organization (WHO) and the United Nations' Sustainable Development Goals (SDGs), particularly SDG 3 (Good Health and Well-Being), emphasize the importance of reducing neonatal mortality through accessible and sustainable healthcare interventions (WHO, 2015). Solar-powered LED phototherapy systems offer a promising solution by leveraging renewable energy to provide uninterrupted treatment, reducing operational costs, and minimizing environmental impact.

Previous studies have explored the feasibility of solar-powered medical devices in low-resource settings. For instance, Abioye and Abiodun (2019) developed a solar-powered phototherapy device using fluorescent lamps, demonstrating the potential for renewable energy in neonatal care. However, their system lacked integrated diagnostic tools, such as bilirubin or temperature monitoring, limiting its clinical utility. Similarly, a study by Slusher et al. (2015) evaluated solar-powered filtered sunlight devices in Nigeria, reporting efficacy in reducing bilirubin levels but highlighting safety concerns due to inconsistent light intensity and UV exposure risks. LED-based systems have been shown to outperform these alternatives in terms of energy efficiency and safety (Vreman *et al*., 2008). For example, a randomized controlled trial by Kumar et al. (2010) found that LED phototherapy achieved faster bilirubin reduction compared to compact fluorescent tubes, with no significant difference in adverse effects.

The integration of diagnostic tools, such as non-invasive transcutaneous bilirubin measurement, further enhances the utility of phototherapy systems in rural settings. Transcutaneous bilirubinometry, which measures bilirubin levels through the skin using reflectance spectroscopy, reduces the need for invasive blood tests, improving patient comfort and reducing costs (Maisels *et al*., 2004). However, existing devices are often expensive and require calibration for diverse skin types, posing challenges in low-resource settings (Wong *et al.*, 2002). Temperature monitoring is equally critical, as neonates, particularly preterm infants, are susceptible to hypothermia or hyperthermia during phototherapy (Aydemir *et al.*, 2014). The incorporation of real-time temperature sensors and alarm systems can mitigate these risks, ensuring safe treatment delivery.

The environmental impact of healthcare technologies is an emerging concern, particularly in the context of global efforts to achieve carbon neutrality. Traditional phototherapy devices, reliant on grid electricity or diesel generators, contribute to greenhouse gas emissions, undermining sustainability goals (Kalogirou, 2022). Solar-powered systems, by contrast, align with environmentally sustainable practices by harnessing renewable energy, reducing operational costs, and minimizing carbon footprints. The use of locally sourced materials in device fabrication further enhances affordability and scalability, addressing supply

chain challenges in rural areas (Olatomiwa *et al.*, 2015).

This study aim was to address the multifaceted challenges of neonatal jaundice management in rural settings by designing and fabricating a solar-powered LED phototherapy system. The specific objectives are to:

(1) design and fabricate a solar-based UPS for continuous phototherapy,
(2) develop a temperature monitoring and alarm system,
(3) create a non-invasive transcutaneous bilirubin measurement system, and
(4) produce an affordable phototherapy system using locally sourced materials suitable for rural communities.

2.0 Materials and Methods

2.1 Materials

The materials used for this work are listed as shown in Table 1.

2.2 Methods

The methods used for the design and fabrication of the solar based phototherapy machine consist of three different processes namely:

1. Circuit design and implementation
2. Software design and implementation
3. Fabrication of casing/ bed

2.2.1 Circuit Design and Implementation

The complete circuit of the solar based phototherapy machine is shown as in Figure 1 below. It consists of various units such as:

i. Uninterruptable Power Storage Unit
ii. Temperature Sensing Unit
iii. Transcutaneous Bilirubinometry
iv. Control Unit
v. Switching and Alarm Unit
vi. Display Unit

2.3 Uninterruptable Power Storage Unit

The uninterruptible power storage unit in the solar-powered LED phototherapy system ensured the continuous and reliable power delivery to the neon LEDs for treatment of neonatal jaundice. The unit integrated a 100W monocrystalline solar panel, charge controller, 12V, 50Ah lithium-ion battery, inverter circuit with the 220VAC output. The solar panel harvests sunlight at an optimal 19.12V and 5.23A to charge the battery during approximately 12 hours of effective sunlight through a charge controller circuit. The charge controller uses PWM technology and a microcontroller-driven MOSFET with optocoupler to regulate charging and prevent overcharging or over-discharging of the deep-cycle battery which stores energy for up to 12 hours in operation. The battery is then connected to an inverter circuit which converts the stored DC voltage to AC voltage. The system block diagram is shown as Figure 2 and the circuit diagram of the uninterruptible power storage unit is shown as in Figure 3.

Table 1: List of materials

S/No	Component	Type	Quantity
1.	Resistor	Variable resistor 10kΩ	2
		10k	10
		1kΩ	8
		100Ω	5
2.	Capacitor	22pF	1
		220µF	2
3.	Diode	2N4001	3
4.	Comparator	LM393	2
5.	Transistor	NPN	2
		PNP	1
6.	Voltage regulator	7805	1
7.	LED lights	Neon	4 yards

8.	Vero Board	Small	1
9.	Liquid Crystal Display (LCD)	16x2	1
10.	Relay	12V	1
11.	Battery	12V, 7A	2
12.	Switch	Toggle	1
13.	Microcontroller	PIC	1
14.	Wire	Connecting/ Jumper	3 yards
		2.5mm wire	5 yards
15.	Soldering Iron	Plastic	1
16.	Soldering Bits	small	2
17.	Soldering Lead	small	1 roll
18.	Buzzer (Alarm)	small	1
19.	Inverter	150W	1
20.	Dimmer Switch		1
21.	Crystal Oscillator		1
22.	Paxpex material		1
23.	Galvanized sheet		15MS
24.	Tire/ roller	Medium	4
25.	Baby foam		1
26.	7 pins IC Sockets		1
27.	28 pins IC Sockets		1
28.	Solar Panel	100 Watts	1

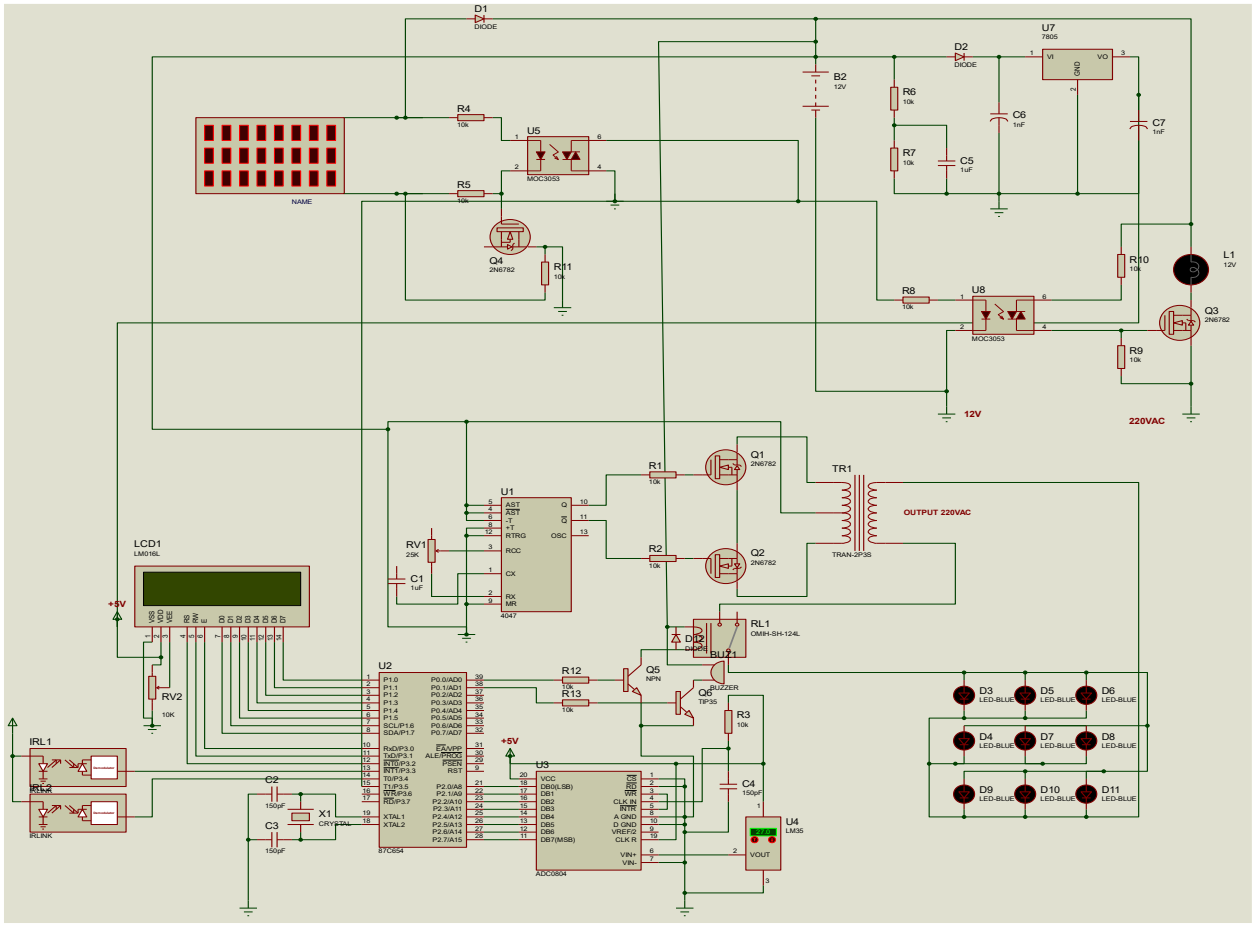

Figure 1: The complete circuit of the solar based phototherapy machine

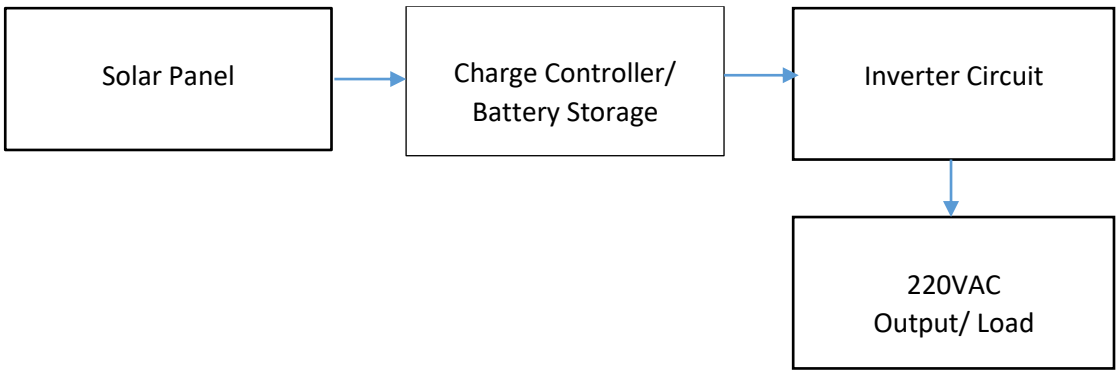

Figure 2: the block diagram of uninterrupted power supply unit

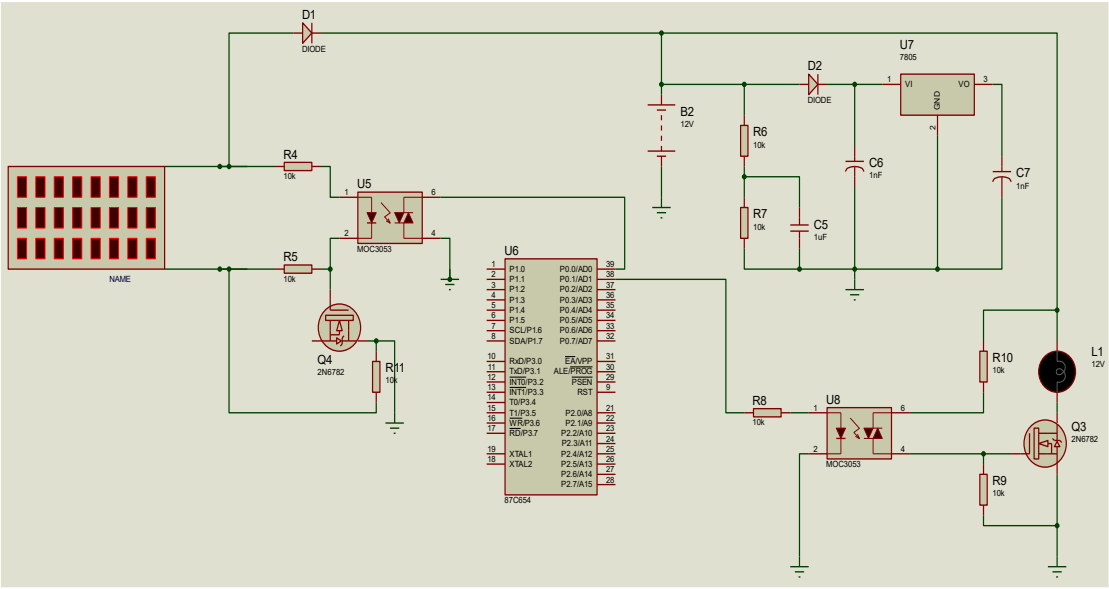

Figure 3: Circuit diagram of uninterruptible power storage unit

The operation of an inverter circuit involves the conversion of direct current (DC) into alternating current (AC), a process essential for various applications such as solar power systems, uninterruptible power supplies (UPS), and electric vehicles. At its core, the inverter circuit takes a DC input from a power source, which could be a battery or a solar panel array, storing energy from renewable sources or serving as a backup system as shown in Figure 4.

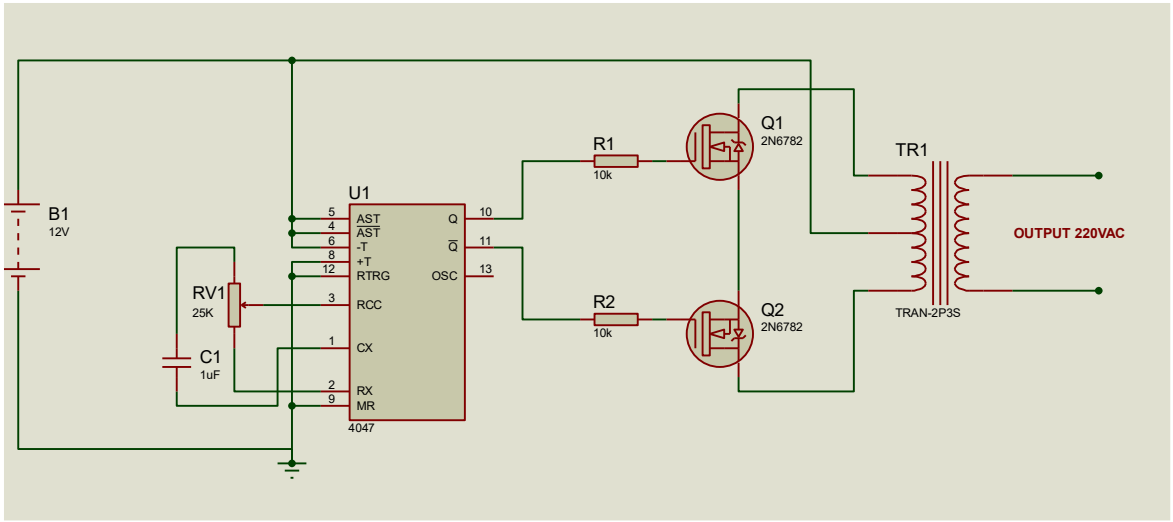

Figure 4: Circuit diagram of Inverter

In the typical configuration utilizing the CD4047B IC, the CD4047B serves as a versatile CMOS IC, providing precise timing signals for controlling switching devices such as MOSFETs D1 and D2. The CD4047B IC is configured in the astable multivibrator oscillator mode, with its Pin 7 (CLK) connected to an external resistor-capacitor (RC) network to set the oscillator frequency. This network determines the frequency of the oscillator, which controls the switching frequency of the inverter, allowing for the generation of the desired AC waveform. The two oscillating outputs are out of phase that is Pin 10 and Pin 11, the 50K variable resistor determine the frequencies of the oscillations.

The waveform across all the above three outputs of 4047 is an ideal square wave. Each single output waveform cycle can be calculated through the equation: T = 4.4RC seconds.

The output frequency of the IC can be determined using the equation 1.

$$f = 1/4.4RC \quad (1)$$

Setting f = 50Hz and C = 2.2uF, R can be calculated as:

$$50Hz = \frac{1}{4.4 \times 2.2 \times 10^{-6} \times R}$$

$$R = \frac{1}{0.000484} = 2066.12\Omega$$

Therefore, 2 kΩ resistor and 100Ω variable resistor connected in series were used to achieve 2066.12 Ω.

The power MOSFETs (IRF3205) amplifies each half of the alternating voltage produced by the oscillator to the output power transformer which steps up the voltage from 12V DC to 220V AC. However, one can increase the output power to up to 1000W or more by adding more power MOSFETs in parallel, greater power transformer, and larger battery power bank. Once the AC waveform is generated, it passes through a transformer as an AC voltage output. The transformer serves to step up or step down the voltage level as needed for the specific application. In grid - tied inverters, the transformer may also provide isolation between the inverter output and the grid, ensuring safety and compatibility with existing power infrastructure.

I. Temperature Sensing Unit

The temperature monitoring unit in the solar-powered LED phototherapy system ensures neonatal safety by continuously monitoring the temperature in and around the phototherapy machine using an LM35 sensor and an ADC0804 analog-to-digital converter connected to a microcontroller as shown in Figure 5. The LM35 sensor with its linear 10 mV/°C output, low 60 µA current draw, and ±0.5°C accuracy at 25°C detects temperatures within a −55°C to +150°C range and sends analog voltage signals to the ADC0804 integrated circuit (IC) which converts these signals into an 8-bit digital output with a 19.53 mV step size at a 5V reference voltage (or 7.84 mV at a 2V reference) enabling 256 discrete measurement levels. The microcontroller processes this digital data to display the temperature on an LCD screen and triggers an alarm while switching off the neon LEDs if the temperature exceeds 41°C, preventing hyperthermia risks in neonates; the ADC0804's compatibility with microcontrollers, 135 ns access time, and internal clock (or external RC circuit) ensure efficient and accurate signal conversion, making the unit critical for maintaining safe thermal conditions during phototherapy in rural settings.

II. Transcutaneous bilirubinometry

The measurement of Bilirubin was designed using IBM block diagram for the development of Infant Bilirubin Meter as shown in Figure 6.

The input to the PIC microcontroller is obtained from two infra-red sensor which receives the lights that reflects from the sample (baby finger) through 2 LED. The light is passed through the sample inside the black box in order to have persistence of lights. The outputs are LCD display, LEDs (green and red) and buzzer that will demonstrate the condition of the disease. The circuit diagram is shown as in Figure 7.

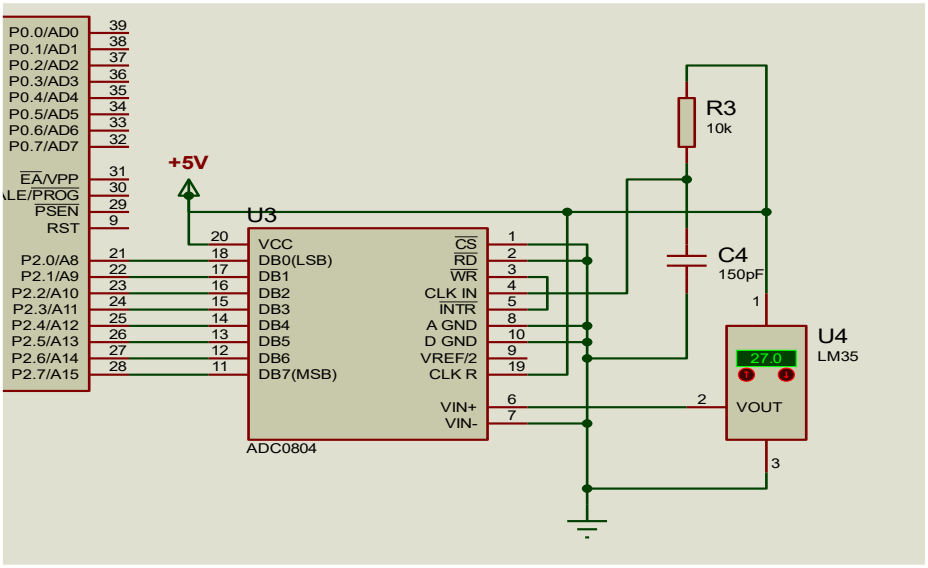

Figure 5: Circuit Diagram of Temperature Monitoring Unit

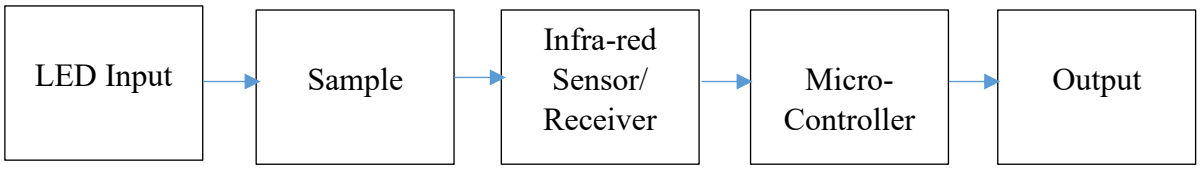

Figure 6: Block diagram of transcutaneous bilirubinometer

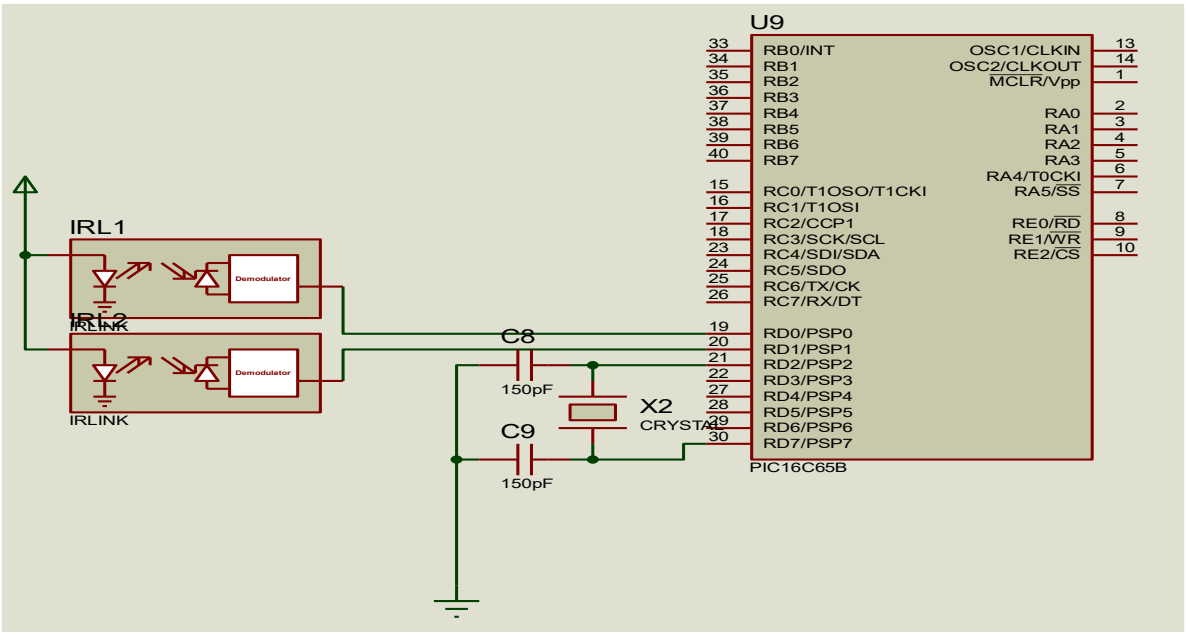

Figure 7: Circuit diagram transcutaneous bilirubinometer

III. Control Unit

The control unit was designed with a PIC18F26K22 microcontroller. Microcontroller is a type of integrated circuits designed to govern a specific operation in an embedded system. A typical microcontroller includes a processor, memory and input/output (I/O) peripherals on a single chip. This Microcontroller is made up of CPU, RAM, ROM, I/O Ports. PIC18F26K22 Microcontroller is the preferred microcontroller in this project. This is because there are more I/O pins (Mazidi *et al*., 2008). The circuit diagram is shown as in Figure 8.

IV. Switching and Alarm Unit

The switching area of the circuit consists of a transistor switches, relay and an alarm/buzzer. The configuration of the circuit is shown as in Figure 9 below. The AC LED lights and the Buzzer are been driven by the microcontroller.

This was achieved by configuring transistors to operate in two of its three modes of operation. The transistor was biased to go into saturation when it is latched by the microcontroller, and go into cut-OFF mode when de-latched. For this to happen, the current through the collector must be far less than beta multiplies by the base current.

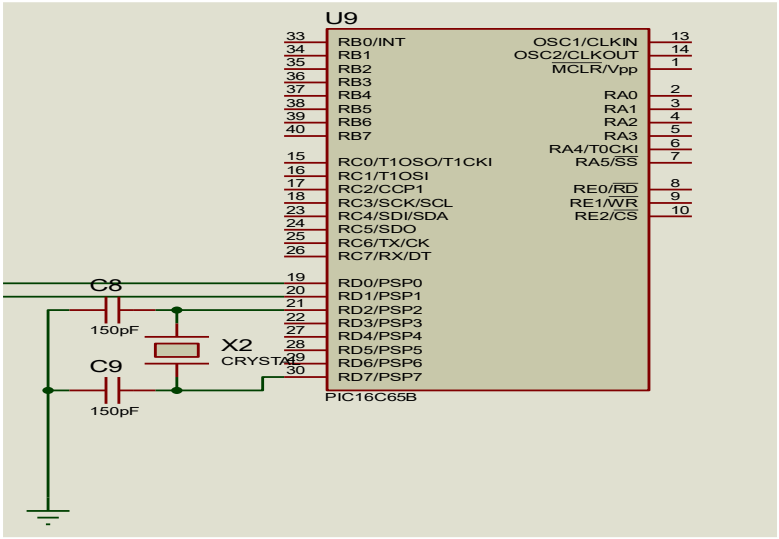

Figure 8: Schematic of Control Unit

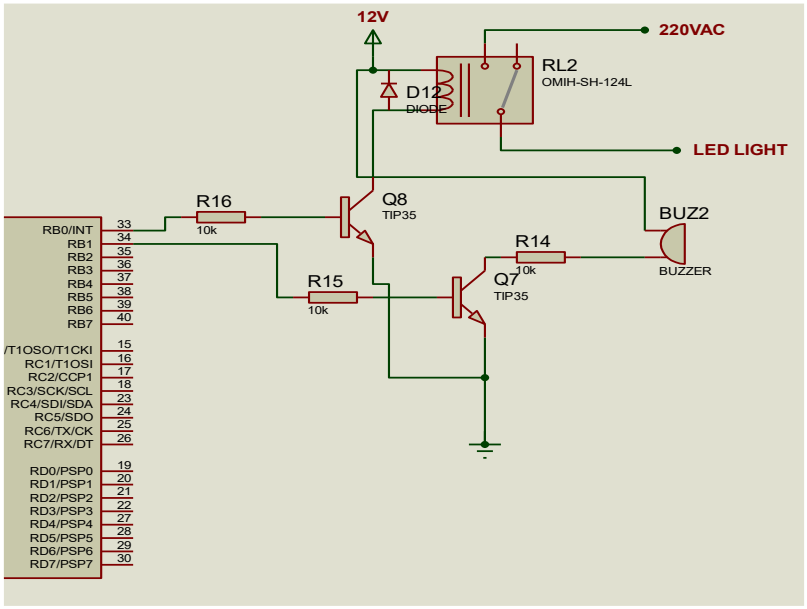

Figure 9: Configuration of the Switching circuit

Relays switches, popularly known as relays are used for switching operations. The relays have contact point which form the normally open (NO) and the normally closed (NC) switches. It has an energizing coil through which the switching contacts can be pulled together or drawn apart to accomplish the NO and NC effects. When a current passes through the coil of the relay, the metal core becomes magnetized and attracts a strip of metal which closes the contacts that form the normally open switch. At this point the normally closed terminal opens. Removing the energizing voltage demagnetize the metal core which then releases the metal strip to open the NO terminal and close the NC terminal again. Thus, the relay contacts can be opened or closed by simply applying or removing the energizing voltage as required. The LED light was connected to the NC of the relay when energized by the microcontroller it

switch to NO open and light will come ON. Any other situation of high temperature will turn the light OFF.

The collector current can be expressed as shown in equation 2:

$$IC \ll \beta IB \quad (2)$$

This implies that IB≫ICβ where, β = hFE, known as current gain amplification factor.

Relay data: 12V, 25mA. Transistor Saturation Mode data: $_{(SAT)}$ = 0.80 V, $_{(SAT)}$ = 0.2 V and h_{FE} = 100, R_5 =R_B. Taking Kirchhoff's voltage law (KVL) of C-E loop of Figure 3.13 and making IC the subject of the relation as shown in equation 3:

$$I_C = \frac{12 - V_{CE}}{R} \quad (3)$$

where R is relay resistance

$$R = \frac{\text{Relay voltage}}{\text{maximum relay current}}$$

$$\text{R} = \frac{12\text{V}}{25\text{mA}} = 480\Omega$$

Similarly, taking KVL of B – E

$$I_B = \frac{V_{BB} - V_{CE}}{R_B} = \frac{5.0 - 0.80}{R_B}$$

$$I_B = \frac{4.2}{R_B}$$

Condition for saturation: $I_C < h_{FE} \times \frac{4.2}{R_B}$

Substituting I_C and I_B into the above equations and making R_B subject: R_B< 1kΩ. To ensure that the transistor is operated in saturation mode, a value of 470Ω is suitable for the base resistance (R_B *or* R_5).

Buzzer data: 5V, 25mA. Transistor Saturation Mode data: $V_{BE(SAT)}$ = 0.80 V, $V_{CE(SAT)}$ = 0.2 V and h_{FE} = 100, R_7 = R_B Taking Kirchhoff's voltage law (KVL) of C–E loop of figure 3.13 and making IC the subject of the relation same as equation 3:

$$\frac{12 - V_{CE}}{R}$$

$$R = \frac{\text{Buzzer voltage}}{\text{maximum buzzer current}} \quad (4)$$

$$\text{R} = \frac{12\text{V}}{25\text{mA}} = 480\Omega$$

$$I_C = \frac{12 - 0.2}{480} = 24.5mA$$

Similarly, taking KVL of B – E yields equation 5:

$$I_B = \frac{V_{BB} - V_{CE}}{R_B} \quad (5)$$

$$I_B = \frac{12 - 0.80}{R_B}$$

$$I_B = \frac{11.2}{R_B}$$

Condition for saturation $I_C < h_{FE} \times 11.2R_B$. Substituting I_C and I_B into the above equations and making R_B subject:

$$I_C < h_{FE} \times \frac{11.2}{R_B} = R_B < \frac{11.2}{24} = R_B < 17.5\Omega$$

R_B < 1kΩ. To ensure that the transistor is operated in saturation mode, a value of 470Ω is suitable for the base resistance (R_B *or* R_5).

V. Display Unit

The display unit was design with a liquid crystal display (LCD). The LCD is a dot matrix liquid crystal display that displays alphanumeric characters and symbols. 16X2 LCD digital display has been used in the system to show the room temperature. Liquid Crystal Display screen is an electronic display module and find a wide range of applications. A 16x2 LCD display is very basic module and is very commonly used in various devices and circuits. These modules are preferred over seven segments and other multi segment LEDs. The reasons being: LCDs are economical; easily programmable; have no limitation of displaying special & even custom characters (unlike in seven segments), animations and so on. A 16x2 LCD means it can display 16 characters per line and there are 2

such lines. In this LCD each character is displayed in 5x7 pixel matrix. This LCD has two registers, namely, Command and Data. The command register stores the command instructions given to the LCD. A command is an instruction given to LCD to do a predefined task like initializing it, clearing its screen, setting the cursor position, controlling display etc. The data register stores the data to be displayed on the LCD. The data is the ASCII value of the character to be displayed on the LCD. The circuit diagram is shown as in Figure 10. The display unit shows the temperature level of the surrounding.

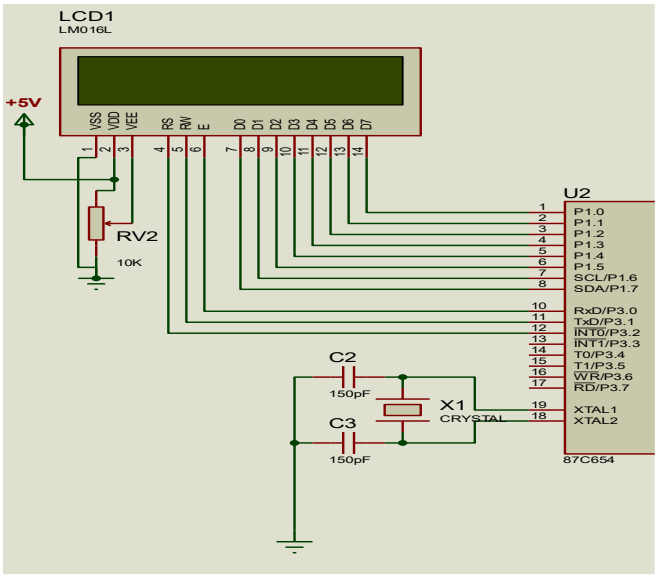

Figure 10: Circuit Diagram of the Display Unit

2.4 Software Design

The software electronic design controls all cell phones, microwaves, network routers, automobiles, and industrial controls all around the world. Each of these embedded systems is unique and highly customized to the specific application as this prototype (solar based phototherapy device) (Lutkevich, 2020). Embedded software is computer software, written to control machines or devices that are not typically thought of as computers, commonly known as embedded systems. It is typically specialized for the particular hardware that it runs on and has time and memory constraints (Lutkevich, 2020). This term is sometimes used interchangeably with firmware (Maurizio, 2014). A precise and stable characteristic feature is that not all functions of embedded software are initiated/controlled via a human interface, but through machine-interfaces instead (Lutkevich, 2020).

Manufacturers build embedded software into the electronics of cars, telephones, modems, robots, appliances, toys, security systems, pacemakers, televisions and set-top boxes, and digital watches, for (Emilio, 2014). This software can be very simple, such as lighting controls running on an 8-bit microcontroller with a few kilobytes of memory with the suitable level of processing complexity determined with a Probably Approximately Correct Computation framework (a methodology based on randomized algorithms) (Alippi, 2014). However, embedded software can become very sophisticated in applications such as routers, optical network elements, airplanes, missiles, and process control systems (Alippi, 2014).

Unlike standard computers that generally use an operating systems such as macOS, Windows or Linux, embedded software may use no operating system. When they do use one, a wide variety of operating systems can be chosen from, typically

a real-time operating system. Code for embedded software is typically written in C or C++, but various high-level programming languages, such as Java, Python and JavaScript, are now also in common use to target microcontrollers and embedded systems (Mazzei et al., 2015). Assembly languages are often used too, especially in booting and interrupt handling. Ada is used in some military and aviation projects (Mazzei et al., 2015).

The microcontroller in embedded systems receives temporary data that is stored in its data memory, where the processor accesses it and employs programme memory instructions to interpret and apply the incoming data. It then utilizes its I/O peripherals for communication and performs the required operation.

Key Components of Microcontrollers in Embedded Systems

(a) **Processor Core:** The controller's primary building block is the CPU. It includes the registers, stack pointer, programme counter, accumulator register, register file, etc. as well as the arithmetic logic unit.

(b) **Memory:** Program memory (microcontroller embedded c programming) and data memory are the two forms of memory found in embedded microcontrollers. The microcontroller's program memory, sometimes referred to as flash memory, is where the code is stored for execution. Data memory, sometimes referred to as RAM, is where the variables and data are stored that the microcontroller needs to function.

Three different types of memories are used to build microcontrollers and microprocessors:

- RAM Memory
- Flash memory
- EEPROM storage

In the memory, program memory and data memory are divided. Data transfers between peripheral devices and the memory are managed by the DMA controller.

(c) **Interrupt Controller:** An interrupt controller provides a programmable governing policy that enables software to select which peripheral or device can interrupt the processor at any particular time by setting the appropriate bits in the interrupt controller registers.

(d) **Timers/Counters:** The majority of controllers have one or more timers and counters. A timer is a kind of clock that is used to record durations of time. A counter is an instrument that records the frequency of a specific event or process with respect to a clock signal.

(e) **Digital I/O:** One of the key characteristics of the microcontroller is its digital I/O. An interface board known as a digital I/O board enables a computer to input and output digital signals simultaneously. There are anywhere from 3 to 90 I/O pins.

(f) **Analog I/O:** Most microcontrollers have integrated analogue to digital converters for analogue I/O.

(g) **Interfaces:** One can download the programme and communicate with the development PC, in general, using the serial interface. Additionally, serial ports provide external peripheral device communication. The majority of controllers come with a range of interfaces, including Ethernet, SPI, SCI, PCI, and USB.

(h) **Debugging Unit:** The process of debugging entails identifying and resolving existing and potential bugs—commonly referred to as "bugs"—in software code that could cause it to behave strangely or crash. Some controllers come with extra hardware

that makes it possible to remotely debug the chip from a PC.

(i) **CPU: Central Processing Unit:** The microcontroller's central processing unit, or CPU, is in charge of carrying out calculations and carrying out instructions. In most cases, it is a low-power, slow CPU designed for embedded devices.

(j) **Peripheral Input/Output (I/O) Devices:** A variety of input/output peripherals on microcontrollers enable them to communicate with the outside world. Pulse width modulation (PWM) outputs, timers, counters, communication interfaces (such as UART, SPI, I2C, and USB), and digital and analogue input/output pins are a few of these.

(k) **Power Control:** For proper operation, microcontrollers need a reliable and steady power source. Voltage regulators and other power management elements are built into the chip to guarantee that the microcontroller receives the proper voltage and current.

In the software implementation part was developed using C+ code for measuring temperature and controlling it according to the user's requirements and displaying the temperature in LCD module. The software includes the reading of various measurements from sensor, converting analog value to digital values, displaying the temperature in the 16X2 LCD display and the program for controlling action. The C+ level programming is done on Visual studio IDE software, the developed program is installed in the ATMega328 microcontroller. The Visual studio IDE combines project management, make facilities, source code editing, program debugging, and complete simulation in one powerful environment it is shown as in Figure 11. The Arduino platform is easy-to-use and helps one to quickly create embedded programs that work. The Arduino editor and debugger are integrated in a single application that provides a seamless embedded project development environment. The Visual studio IDE supports Windows, Mac OS X and also Linux. The circuit diagram has been drawn using Proteus 8.7 software.

2.4.1 Software Design Flow Chart

The flowchart shown in Figure 12 represents the workflow or process of the prototype. A flowchart can also be defined as a diagrammatic representation of an algorithm, a step-by-step approach to solving a task. The flowchart shows the steps as boxes of various kinds, and their order by connecting the boxes with arrows. This diagrammatic representation illustrates a solution model to a given problem. Flowcharts are used in analyzing, designing, documenting or managing a process or program in various fields (Shelly & Vermaat, 2011; Valvano, 2011).

2.5 Fabrication of Metal Frame/Casing

Fabrication is an integral part in creating the phototherapy for neonatal jaundice prototype, where raw materials are transformed into functioning products. The fabrication process itself is versatile, allowing for adaptability and customization to meet various production and industrial requirements. According to Timings (2008) metal fabrication is the creation of metal structures by cutting, bending and assembling processes. It is a value-added process involving the creation of machines, parts, and structures from various raw materials (Timings, 2008).

The fabrication process used in this study include:

I. Cutting is done by sawing, shearing, or chiselling (all with manual and powered variants); torching with handheld torches (such as oxy-fuel torches or plasma torches); and via numerical control (CNC) cutters (using a laser, mill bits, torch, or water jet) (Timings, 2008).

II. Bending is done by hammering (manual or powered) or via press brakes, tube benders and similar tools. Modern metal fabricators use press brakes to coin or air-bend metal sheet into form. CNC-controlled backgauges

use hard stops to position cut parts to place bend lines in specific positions.

III. Assembling (joining of pieces) is done by welding, binding with adhesives, riveting, threaded fasteners, or further bending in the form of crimped seams. Structural steel and sheet metal are the usual materials for fabrication; welding wire, flux and/or fasteners are used to join the cut pieces.

The fabrication comprises or overlaps with various metalworking specialties in this study welding. Welding is a fabrication process whereby two or more parts are fused together by means of heat, pressure or both forming a join as the parts cool. Welding is usually used on metals and thermoplastics but can also be used on wood. The completed welded joint may be referred to as a weldment.

There are three main components needed to create a weld. These are:

1. A heat source such as an electric arc, a flame, pressure, or friction. The most common heat source is an electric arc. An arc is the physical gap between the end of the electrode and the base metal. The physical gap causes heat due to resistance of current flow and arc rays. The arc melts the metals to create the joint.
2. Shielding, which is the use of gas, or another substance to protect the weld from air as the weld is being formed. Oxygen from the air makes welds brittle and porous.
3. Filler material, which is the material used to join to the two pieces together.

Other processes that join metals together include:

4. Brazing is the joining of metals with a filler metal having a melting point above 450°C (842°F), but below the melting point of base metals. The joined metals can be different metals. The joint is not as strong as a welded joint.
5. Soldering is the joining of metals using a filler metal with a melting point below 450°C (842°F). The joined metals can be different metals. The "filler" metals commonly used are lead-tin alloys. The joint is not as strong as a welded joint or a brazed joint. The fabricated design is shown as in Figure 13.

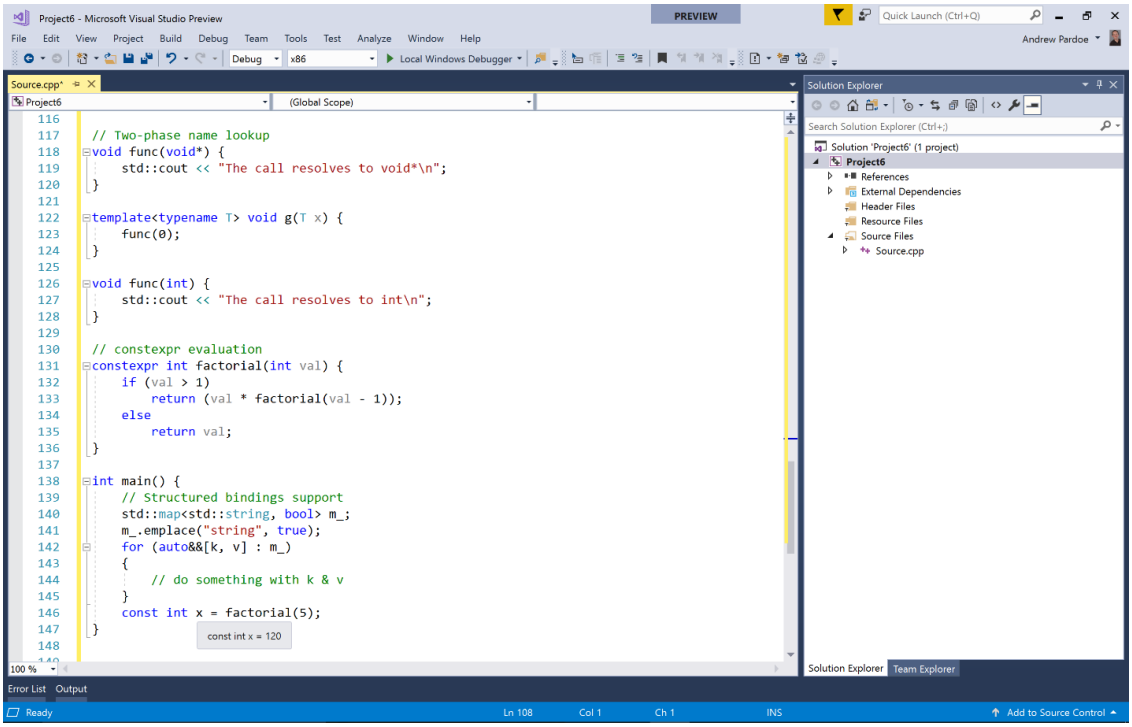

Figure 11: Visual Studio Interface

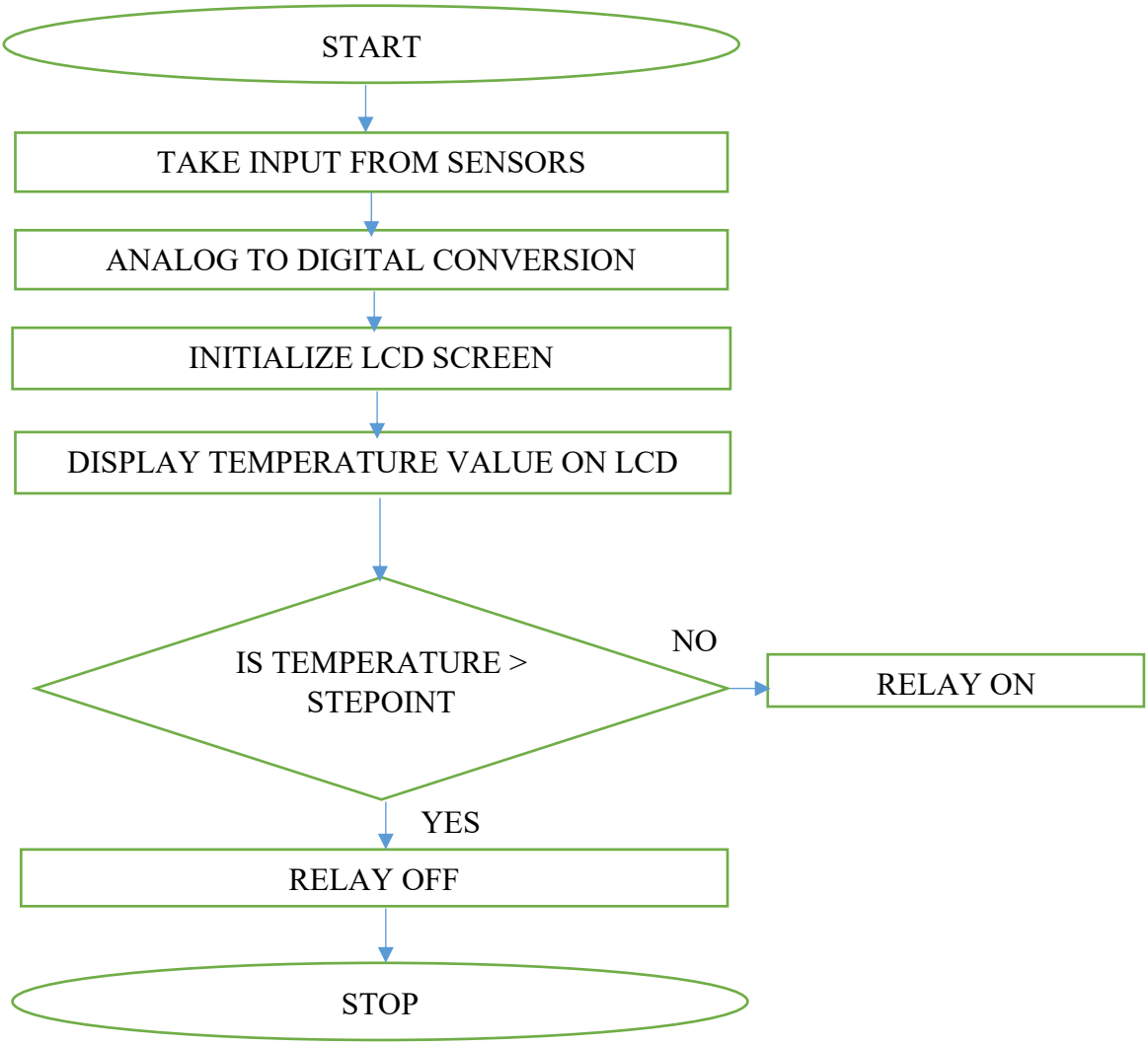

Figure 12: Software Design Flow Chart

3.0 Results

Testing is a necessary activity for verifying and validating the functionality, durability or reliability of a product. A potential design can be subject to mismatches with customer needs, technical design faults, or issues regarding manufacturability and maintainability of the product (Qian *et al*., 2010). Testing is a primary way to identify these problems and therefore is central to product development (PD) (Thomke, 2003). But testing is an expensive and time-consuming process. A critical aspect of the design process is to effectively deploy various testing activities throughout the PD process to assure product quality. Various tests were carried out using multi-metre to test voltage, current, resistance from which computations were made to get various desired parameters such as power etc., photometer was used to measure the light intensity, temperature sensor was used to measure the temperature and the collated data were presented in tables, plates and figures below.

I. Solar Panel Test

The solar panel was tested for functionality by reading their open circuit voltage using a voltmeter. The value of the voltage reading should be positive, and if negative, that implies the probe matching with the solar panel terminals was wrong and should be reversed. The results from various readings repeated for three days are shown in Table 2. A compass was used to determine the best position for the solar panel. According to the study of Kalogirou (2022) solar panels are best installed facing true

south, if in the northern hemisphere, to receive direct sunlight all through the day. The tilt angle was established to be between 10° to 25° for optimum performance of given 15 – 25 V.

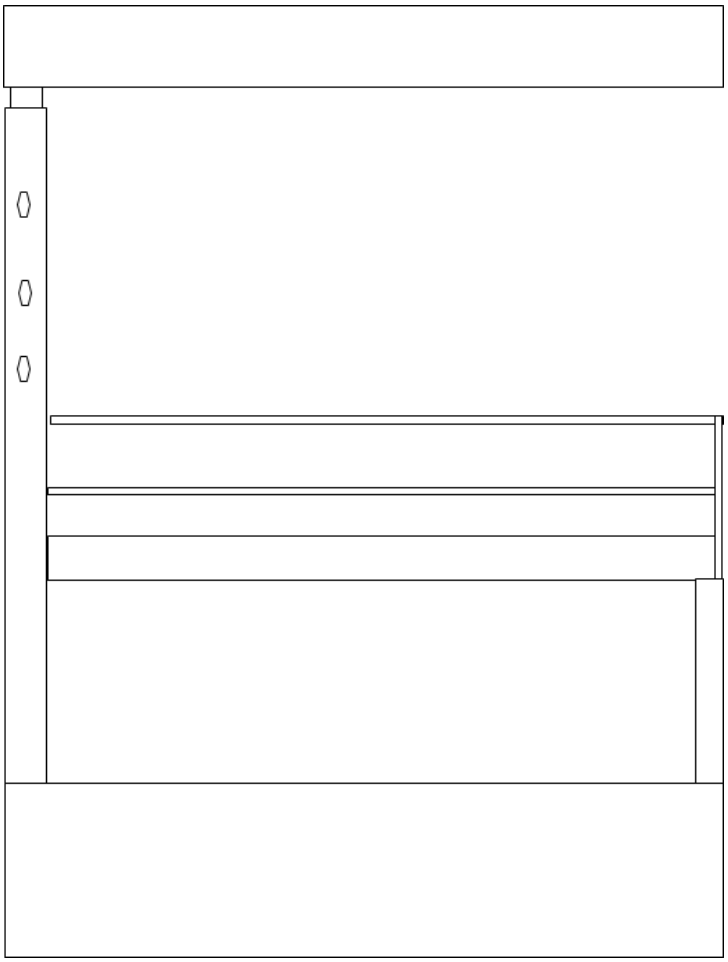

Figure 13: Schematic diagram of Phototherapy casing

Table 2: Solar panel output voltages at different time of the day

Time	DAY 1	DAY 2	DAY 3	MEAN VOLTAGE
05:00 AM	0.120	0.110	0.120	0.120
06:00 AM	1.230	1.340	1.441	1.340
07:00 AM	7.890	8.760	9.112	8.591
08:00 AM	11.20	12.10	12.22	11.84
09:00 AM	13.41	14.20	13.82	13.81
10:00 AM	15.01	16.22	15.65	15.63
11:00 AM	16.55	17.02	17.01	16.86
12:00 PM	17.05	17.23	17.12	17.13
01;00 PM	17.56	17.47	17.65	17.56
02:00 PM	17.46	17.65	17.44	17.52
03:00 PM	17.71	17.62	17.23	17.52
04:00 PM	17.44	17.45	17.55	17.48
05:00 PM	16.23	16.43	16.21	16.29
06:00 PM	14.33	14.65	13.54	14.17
07:00 PM	1.230	2.110	3.011	2.121

II. Battery Test

Functionality tests were carried out on the battery; the expected voltage capacity of the battery at idle state should not be less than 11.8V – 12.5V, which implies it is in good working condition. The battery was measured with digital multi-meter which gave 12.34V, the battery was satisfactory and in good condition. The battery was also tested on load at different hourly intervals results is shown as in Table 3.

Table 3: Results of Functionality tests battery

Time	Battery Voltage (V_{DC})	Inverter Output Voltage (V_{AC})
07:00 AM	12.4	220.0
08:00 AM	12.4	220.1
09:00 AM	12.3	219.2
10:00 AM	12.3	219.2
11:00 AM	12.3	219.1
12:00 PM	12.2	219.1
01:00 PM	12.2	218.7
02:00 PM	12.2	218.7
03:00 PM	12.1	218.6
04:00 PM	12.1	218.6
05:00 PM	12.1	218.4
06:00 PM	12.0	217.5
07:00 PM	11.9	217.3

III. Results on Charge Control and Inverter Test

For the safety of the charge controller and batteries, batteries should be connected to the charge controller first before the solar panels are connected to the charge controller and vice versa when uninstalling the system. The battery terminals were connected to the input terminals of the inverter, and the output of the inverter was connected to the loads. The inverter was connected to the terminals of the 12V battery source to match its voltage rating of 12V and powered ON, and the AC power output at no load was read using a voltmeter the result showed 220VAC output as shown in Figure 14.

IV. Results of Load Performance Test

The solar powered phototherapy system was tested for functionality using the LED lights and other components joined together. The load was able to stay for 12 hours straight in continuous load condition.

V. Results of Temperature Sensor Test

The experiment was conducted under normal room temperature. The temperature of the system was calibrated to stay at room temperature on START 37.6˚C. The measurement results of the temperature sensor are shown in Table 4. The error range of temperature sensing monitoring is within±1◦C, which meets the temperature sensing monitoring design requirements.

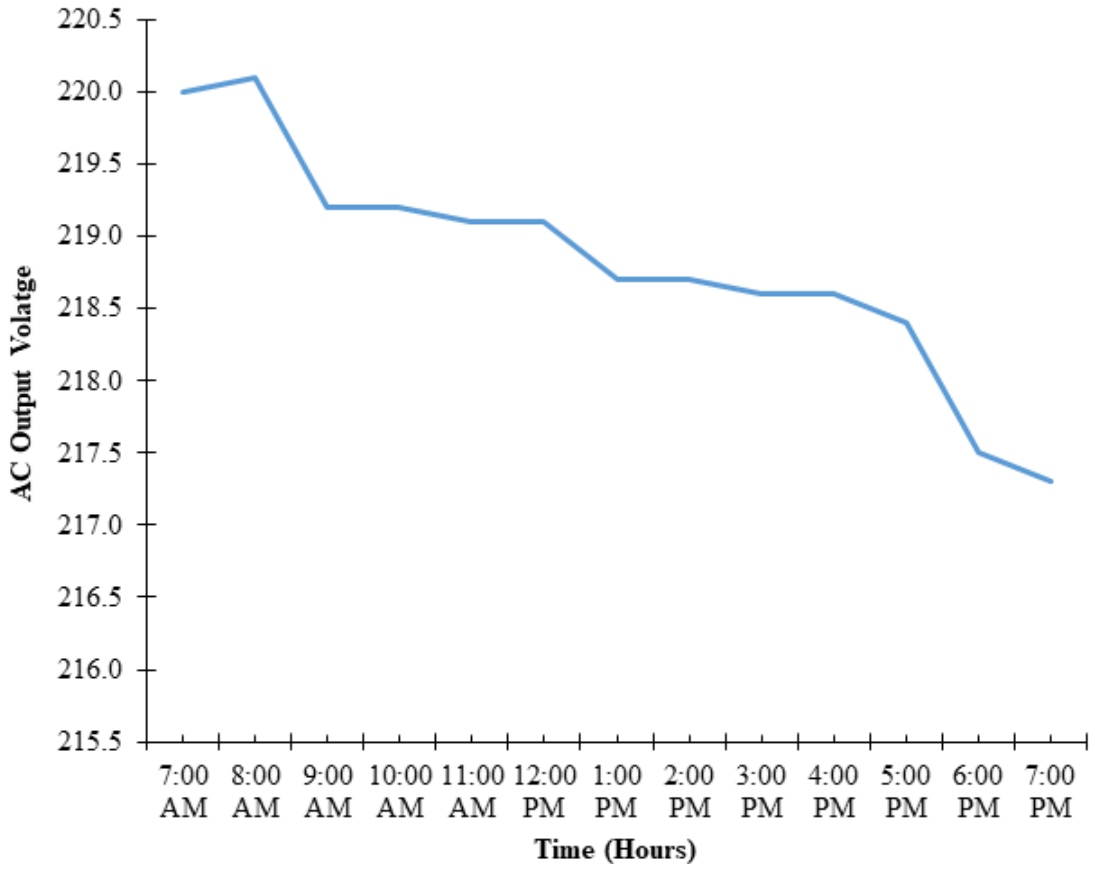

Figure 14: AC power output voltage with respect to time

Table 4: The measurement results of the temperature sensor

Temperature Level	Alarm	LED Light
37.2°C	OFF	ON
38.1°C	OFF	ON
40.1°C	OFF	ON
44.4°C	ON	OFF

VI. Results of Bilirubin Meter Test

The test was carried out by placing a finger or hand through IR device the output was indicted by the LED as shown in Table 5. The results from Table 5 indicated that there was no bilirubin in the sample.

VII. Results of LED Irradiance Test

The irradiance of the LED lights was measured using a radiometer at various distances from the light source. The results as shown in Table 5 indicated that the device delivered irradiance levels suitable for standard phototherapy (>8-10 µW/cm²/nm) at a distance of 15-20 cm. The irradiance did not reach levels classified as intensive phototherapy (>30 µW/cm²/nm).

4.0 Discussion

The system was able to stay ON for about 12 hours continuously powering the phototherapy lights. This can carry many sessions of phototherapy. The device in lasted longer than that by Oyedun (2011) whose inverter system lasted for 4 hours. This may be because of other loads applied to the system. According to Arnold et al., (2020) intermittent phototherapy allows babies to come out of phototherapy for segments of time. In some cases, phototherapy is

scheduled or "cycled," i.e. a baby might be scheduled to go under phototherapy lights for 15 minutes every hour, and then have a 45-minute scheduled "break" before it resumes. In other cases of intermittent phototherapy, light treatment is prescribed for a certain number of hours each day, but is not put on a strict schedule or regimen. For example, parents might be told their baby should be under phototherapy lights for 14 out of every 24 hours, but these 14 hours can be scheduled for whenever it works best for a newborn and their family (Madden, 2024). In a 2015 study of 75 newborns in India, phototherapy using a 12 hour ON/12 hour OFF regimen was found to actually be superior to continuous phototherapy. This also indicate that the prototypes can serve it purpose of uninterruptable power supply during phototherapy for neonates. Per a more recent meta-analysis of intermittent phototherapy, which included 716 newborns and was published in 2021, intermittent phototherapy was found to be as effective as and safer than continuous phototherapy.

Table 5: Results of Bilirubin Meter

S/No	Indicator	Indication	Results
1	Green	Normal	ON
2	Red	Positive/High	OFF
3	Blue	Positive/ Low	OFF

Table 6: LED Irradiance Measurements

Distance from Light Source (cm)	Spectral Irradiance (μW/cm²/nm)
10	22.5
15	15.1
20	9.8
25	6.2

Madden (2024) disclosed the following benefits of intermittent phototherapy: increased time that mother-baby dyads can be in direct skin-to-skin contact, improved breastfeeding outcomes, better thermoregulation, lights that can be adjusted with babies' natural circadian rhythms, and reduced length of treatment.

The temperature monitoring and alarm system worked perfectly sounding the alarm at 38.5ºC - 44.4ºC. This is because most, Aydemir et al., (2014) disclosed that mean body temperature of baby should be between ≥ 37.5 °C and BT ≥ 38 °C during phototherapy and his study found that all baby BT measurements were <37.5 °C during phototherapy. Their study highlighted the significance of maintaining a baby's body temperature between 37.5°C and 38°C during phototherapy sessions. By incorporating an alarm system triggered within a narrow temperature range, this design ensures prompt detection of deviations from the desired temperature range, allowing for timely intervention to prevent potential complications associated with overheating or hypothermia in newborns undergoing phototherapy. The efficacy of the temperature monitoring and alarm system is demonstrated by its ability to detect deviations from the recommended temperature range accurately. The findings of Aydemir et al. (2014) further validate the importance of maintaining optimal body temperature during phototherapy, as their study indicated that all baby body temperature measurements were below 37.5°C during the

treatment. Therefore, the alarm system's functionality within the specified temperature range reinforces its utility in safeguarding newborns undergoing phototherapy, ensuring their comfort and safety throughout the treatment process.

The device was able measure bilirubin levels at three categories namely normal, positive/ High and positive / Low. This result was similar to the study of Baharuddin et al., (2010) which portable and economical bilirubin meter successfully measured the bile pigments level via IR sensor using PIC microcontroller, the system effectively detects three conditions which are normal, mild and critical jaundice in neonates. Detecting the levels of bilirubin during phototherapy in neonates is paramount in ensuring their well-being and preventing potential complications. Monitoring bilirubin levels allows healthcare providers to assess the severity of jaundice in newborns. High levels of bilirubin can lead to a condition called hyperbilirubinemia, which, if left untreated, can result in kernicterus, a rare but serious neurological disorder. By regularly measuring bilirubin levels during phototherapy, healthcare professionals can track the effectiveness of the treatment and ensure that bilirubin levels are decreasing within safe limits. Secondly, detecting bilirubin levels during phototherapy enables healthcare providers to adjust the treatment regimen as needed. Different newborns may respond differently to phototherapy, and factors such as the intensity and duration of light exposure need to be carefully monitored and adjusted based on the individual baby's response and bilirubin levels (Ansong-Assoku *et al*., 2023). Close monitoring allows healthcare providers to optimize the phototherapy treatment to achieve the desired reduction in bilirubin levels while minimizing potential side effects. Finally, monitoring bilirubin levels during phototherapy helps prevent overexposure to light. While phototherapy is generally considered safe, prolonged exposure to the lights used in treatment can potentially cause skin damage and other complications. By regularly assessing bilirubin levels, healthcare providers can ensure that phototherapy is discontinued once bilirubin levels have decreased to a safe range, minimizing the duration of exposure to the lights and reducing the risk of adverse effects (Horn *et al*., 2021).

The system cost ₦450, 000 while other phototherapy device with bilirubin meter cost about ₦1, 200, 000. The affordability of the system facilitates its adoption and implementation in rural healthcare settings, where budget constraints often hinder access to vital medical equipment. By offering a more cost-effective alternative, the system enhances the capacity of healthcare providers in rural communities to deliver quality care to newborns with jaundice. Moreover, the reduced cost opens up opportunities for community health centers and smaller clinics to invest in phototherapy equipment, thereby decentralizing access to neonatal care and reducing the need for patients to travel long distances to access specialized medical facilities.

The effectiveness of phototherapy at converting bilirubin into configurational isomers, structural isomers, and photooxidation products is determined by the dose of phototherapy provided to the infant. The dose of phototherapy depends on several factors, including the spectral wave length of light, the spectral irradiance delivered to the infant’s skin, and the total spectral power (average spectral irradiance delivered across the surface area of the infant). Light in the blue region of the spectrum, near 460 nm, is most strongly absorbed by bilirubin. However, only light that penetrates the skin and is absorbed by bilirubin provides the needed photochemical effect. Tissue penetration increases as the wavelength of the light increases. Thus, one must balance the use of a higher wavelength of light, which more readily penetrates tissue, with the use of a wavelength

that is more readily absorbed by bilirubin, which may penetrate less deeply. With this in mind, light in the 460-490 nm wavelength is probably the most effective for use during phototherapy (Arnold et al., 2020). The dose of phototherapy, in $\mu W/cm^2$ per nm, should be measured during phototherapy using a commercially available radiometer. These devices typically measure the spectral irradiance of phototherapy in the 425-475 or 400-480 nm band wavelength. The radiometer used to measure irradiance should be the one recommended by manufacturer of the light source. Due to variance in the strength of phototherapy over the surface of the infant, and because measurements of spectral irradiance can differ greatly depending on where on the infant the measurement is made, taking several measures in different locations on the infant and averaging the values is important (Arnold et al., 2020).

The irradiance measurements confirmed that the device delivers light intensity within the range for standard phototherapy (>8-10 $\mu W/cm^2/nm$) at a recommended distance of 15-20 cm from the infant. However, it did not achieve the higher irradiance levels (>30 $\mu W/cm^2/nm$) required for intensive phototherapy. This indicates an area for improvement in future design iterations, potentially by optimizing the LED array or its configuration.

The three major factors that affect the dose of phototherapy include the irradiance of light used, the distance from the light source, and the amount of skin exposed. Standard phototherapy is provided at an irradiance of 8-10 microwatts per square centimeter per nanometer (mW/cm2 per nm). Intensive phototherapy is provided at an irradiance of 30 mW/cm2 per nm or more (430–490 nm). For intensive phototherapy, an auxiliary light source should be placed under the infant. The auxiliary light source could include a fiber-optic pad, a light-emitting diode (LED) mattress, or a bank of special blue fluorescent tubes. Term and near-term infants should receive phototherapy in a bassinet and the light source should be brought as close as possible to the infant, typically within 10-15 cm. However, if halogen or tungsten lights are used, providers should follow the manufacturer recommendation on the distance of the light from the infant to avoid overheating. Preterm infant can be treated in an incubator, but the light rays from the phototherapy device should be perpendicular to the surface of the incubator to minimize light reflectance (Maisel & McDonagh, 2008).

5.0 Conclusion

In conclusion, the solar-based uninterruptible power supply light system showcased remarkable performance, sustaining continuous operation for up to 12 hours, significantly longer than comparable systems reported in literature. This endurance aligns with emerging trends favoring intermittent phototherapy sessions, as intermittent exposure allows for beneficial intervals of skin-to-skin contact, improved breastfeeding outcomes, and better thermoregulation for neonates, as highlighted and corroborated by other studies. The design and fabrication of the temperature monitoring and alarm system demonstrated precision in maintaining optimal body temperature during phototherapy sessions, a crucial factor to ensure the safety and efficacy of treatment. Moreover, the affordability of the system for rural communities provides a practical solution to address healthcare disparities, enabling access to essential phototherapy equipment at a fraction of the cost of traditional devices.

Furthermore, understanding the mechanisms and effectiveness of LED-based phototherapy devices is essential for optimizing treatment outcomes. Proper dosing of phototherapy, measured using appropriate radiometers, ensures effective treatment delivery, with factors such as irradiance, distance from the light source, and extent of skin exposure playing pivotal roles. By adhering to established

protocols for phototherapy administration, healthcare providers can ensure the safe and efficient management of neonatal jaundice, mitigating of the risk of complications and promoting positive clinical outcomes. Overall, these advancements in phototherapy technology underscore the ongoing efforts to improve neonatal care delivery, particularly in resource-limited settings, ultimately enhancing the well-being of newborns and their families.

While the design and fabrication of a solar based cost-effective phototherapy system holds promise for addressing healthcare disparities in rural communities, there are several limitations to consider:

1. The study might have a limited scope, focusing solely on the cost comparison between the new system and existing phototherapy devices with bilirubin meters. Other factors such as maintenance requirements, technical specifications, and long-term sustainability may not have been thoroughly evaluated.
2. The study was not tested on newborns so the effectiveness of the system cannot be measured.
3. While the initial cost of the new system is lower, its long-term cost-effectiveness remains uncertain. Consideration of factors such as durability, maintenance costs, and energy consumption over time is essential to determine the true economic impact of adopting the new system compared to other phototherapy devices.

Based on the findings and discussions presented, several recommendations can be made to enhance the efficacy and accessibility of phototherapy for neonates in both rural and resource-limited settings:

1. Continued efforts are needed to develop and promote affordable phototherapy systems tailored to the needs of rural communities. Collaboration between healthcare professionals, engineers, and policymakers can facilitate the design and fabrication of cost-effective phototherapy devices, ensuring their accessibility and sustainability in resource-constrained settings.
2. Investment in research and innovation is essential to further advance phototherapy technology and improve its effectiveness, safety, and accessibility. Research funding agencies, academic institutions, and industry partners should collaborate to support research initiatives aimed at addressing current challenges and optimizing phototherapy outcomes.

The findings presented in this study make several significant contributions to the existing knowledge base in the field of neonatal care and phototherapy technology:

1. This study demonstrates the feasibility of utilizing solar-based uninterruptible power supply systems to power phototherapy lights for extended periods, thus addressing the challenge of unreliable power supply in rural areas. By achieving a continuous operation of up to 12 hours, this innovation offers a practical solution to ensure uninterrupted phototherapy sessions, contributing to improved treatment outcomes for neonates with jaundice.
2. The development and validation of a temperature monitoring and alarm system designed specifically for use during phototherapy represent a novel contribution to neonatal care technology. By accurately detecting deviations in body temperature within the optimal range, this system ensures timely intervention to prevent complications associated with overheating or hypothermia, thereby improving patient safety and treatment efficacy.
3. The introduction of a cost-effective phototherapy system tailored to the needs of rural communities addresses a critical gap in healthcare access and affordability. By offering a more affordable alternative to traditional phototherapy devices, this

innovation facilitates the decentralization of neonatal care services and promotes equitable access to essential medical equipment, thereby contributing to the reduction of healthcare disparities.

4. The study provides evidence supporting the effectiveness and safety of intermittent phototherapy protocols, particularly in resource-limited settings. By highlighting the benefits of intermittent phototherapy, such as increased maternal-infant bonding, improved breastfeeding outcomes, and reduced treatment duration, this research contributes to optimizing treatment strategies for neonatal jaundice and informs clinical practice guidelines.
5. The study contributes to the understanding of LED-based phototherapy technology by elucidating the mechanisms underlying effective bilirubin conversion and dosing optimization. By emphasizing the importance of balancing light wavelength and intensity, as well as standardizing dosing protocols, this research enhances the efficacy and safety of phototherapy treatment, paving the way for further innovations in neonatal care technology.

References

Abioye, M., & Abiodun, A. E. (2019). Design and analysis of a solar powered phototherapy device. *Journal of Physics: Conference Series*, 1378(3), 032041. https://doi.org-/10.1088/1742-6596/1378/3/032041

Alippi, C. (2014). *Intelligence for embedded systems: A methodological approach*. Springer. https://doi.org/10.1007/978-3-31-9-05278-6

Ansong-Assoku, B., Shah, S. D., Adnan, M., & Ankola, P. A. (2023). Neonatal jaundice. In *StatPearls*. StatPearls Publishing. https://-www.ncbi.nlm.nih.gov/books/NBK567949/

Arnold, C., Tyson, J. E., Pedroza, C., Carlo, W. A., Stevenson, D. K., Wong, R., Dempsey, A., Khan, A., Fonseca, R., Wyckoff, M., Moreira, A., & Lasky, R. (2020). Cycled phototherapy dose-finding study for extremely low-birth-weight infants: A randomized clinical trial. *JAMA Pediatrics*, 174(7), 649–656. https://doi.org/10.1001-/jamapediatrics.2020.0559

Aydemir, O., Soysaldı, E., Kale, Y., Kavurt, S., Bas, A. Y., & Demirel, N. (2014). Body temperature changes of newborns under fluorescent versus LED phototherapy. *Indian Journal of Pediatrics*, 81(8), 751–754. https://doi.org/10.1007/s12098-013-1209-2

Baharuddin, H., Sulong, M. S., Joret, A., Rahman, T. A., & Ismail, N. (2010). Bile pigments detection via IR sensor. In *Proceedings of EnCon2010: 3rd Engineering Conference on Advancement in Mechanical and Manufacturing for Sustainable Environment* (pp. 1–10). Kuching, Sarawak, Malaysia.

Bhutani, V. K., Zipursky, A., Blencowe, H., Khanna, R., Sgro, M., Ebbesen, F., Bell, J., Mori, R., Slusher, T. M., Fahmy, N., Paul, V. K., Du, L., Okolo, A. A., de Almeida, M. F., Olusanya, B. O., Kumar, P., Cousens, S., & Lawn, J. E. (2013). Neonatal hyperbilirubinemia and Rhesus disease of the newborn: Incidence and impairment estimates for 2010 at regional and global levels. *Pediatric Research*, 74(Suppl 1), 86–100. https://doi.org/10.1038/pr.2013.208.

Chang, P. W., Kuzniewicz, M. W., McCulloch, C. E., & Newman, T. B. (2017). A clinical prediction rule for rebound hyperbilirubinemia following inpatient phototherapy. *Pediatrics*, 139(3), e20162896. https://doi.org/10.1542/peds.-2016-2896

Diala, U. M., Wennberg, R. P., Abdulkadir, I., Farouk, Z. L., Zabetta, C. D. C., Omoyibo, E., Emokpae, A., Aravkin, A., Toma, B., Oguche, S., Slusher, T. M., & On behalf of

the Stop Kernicterus in Nigeria (SKIN) study group. (2018). Patterns of acute bilirubin encephalopathy in Nigeria: A multicenter pre-intervention study. *Journal of Perinatology*, 38(7), 873–880. https://doi.org/10.1038/s41372-018-0094-y

Emilio, M. (2014). *Embedded systems design for high-speed data acquisition and control.* Springer. https://doi.org/10.1007/978-3-31-9-06865-7

Ennever, J. F. (1990). Blue light, green light, white light, more light: Treatment of neonatal jaundice. *Clinics in Perinatology*, 17(2), 467–481.

Horn, D., Ehret, D., Gautham, K. S., & Soll, R. (2021). Sunlight for the prevention and treatment of hyperbilirubinemia in term and late preterm neonates. *Cochrane Database of Systematic Reviews*, 7(7), CD013277. https://doi.org/10.1002/14651858.CD013277.pub2

Kalogirou, S. A. (2022). Solar thermal systems: Components and applications-Introduction. In *Comprehensive Renewable Energy* (2nd ed., Vol. 1–3, pp. 1–25). Elsevier. https://doi.org/10.1016/B978-0-12-819727-1.00001-9

Kumar, P., Murki, S., Malik, G. K., Chawla, D., Deorari, A. K., Karthi, N., Subramanian, S., Sravanthi, J., Gaddam, P., & Singh, S. N. (2010). Light emitting diodes versus compact fluorescent tubes for phototherapy in neonatal jaundice: A multi-center randomized controlled trial. *Indian Pediatrics*, 47(2), 131–137. https://doi.org-/10.1007/s13312-010-0020-7

Lutkevich, B. (2020, April 24). Embedded system. In *IoT Industry and Vertical Markets*. TechTarget. https://www.techtarget.com/iota-genda/definition/embedded-system.

Madden, J. (2024). Intermittent phototherapy. NeoLight. https://theneolight.com/inter-mittent-phototherapy/

Maisels, M. J., & McDonagh, A. F. (2008). Phototherapy for neonatal jaundice. *The New England Journal of Medicine*, 358(9), 920–928. https://doi.org/10.1056/NEJMct070-8376

Maisels, M. J. (2005). Jaundice. In M. G. MacDonald, M. M. K. Seshia, & M. D. Mullett (Eds.), *Neonatology: Patho-physiology and Management of the Newborn* (6th ed., pp. 768–846)

Martins, B. M., Carvalho, M., Moreira, M. E., & Lopes, J. M. (2007). Efficacy of new microprocessed phototherapy system with five high intensity light emitting diodes (Super LED). *Jornal de Pediatria*, 83(3), 253–258. https://doi.org/10.2223/JPED.1623

Mazidi, M. A., McKinlay, R. D., & Causey, D. (2008). *PIC microcontroller and embedded systems: Using Assembly and C for PIC18.* Pearson India.

Mazzei, D., Montelisciani, G., Baldi, G., & Fantoni, G. (2015). Changing the programming paradigm for the embedded in the IoT domain. In *2015 IEEE 2nd World Forum on Internet of Things (WF-IoT)* (pp. 239–244). IEEE. https://doi.org/-10.1109/WF-IoT.2015.7389059

Mitra, S., & Rennie, J. (2017). Neonatal jaundice: Aetiology, diagnosis, and treatment. *British Journal of Hospital Medicine*, 78(12), 699–704. https://doi.org/-10.12968/hmed.2017.78.12.699

Muchowski, K. E. (2014). Evaluation and treatment of neonatal hyperbilirubinemia. *American Family Physician*, 89(11), 873–878.

Olatomiwa, L., Mekhilef, S., Huda, A. S. N., & Ohunakin, O. S. (2015). Economic evaluation of hybrid energy systems for rural

electrification in six geo-political zones of Nigeria. *Renewable Energy*, 83, 435–446. https://doi.org/10.1016/j.renene.2015.04.057

Olusanya, B. O., Emokpae, A. A., Zamora, T. G., & Slusher, T. M. (2014). Addressing the burden of neonatal hyperbilirubinaemia in low- and middle-income countries. *The Lancet Global Health*, 2(12), e689–e690. https://doi.org/10.1016/S2214-109X-(14)70326-9

Oyedum, O. (2011). *Design and implementation of off-grid solar inverter for residential application.* Niger State, Nigeria.

Seidman, D. S., Moise, J., Ergaz, Z., Laor, A., Vreman, H. J., Stevenson, D. K., & Gale, R. (2003). A prospective randomized controlled study of phototherapy using blue and blue-green light-emitting devices, and conventional halogen-quartz phototherapy. *Journal of Perinatology*, 23(2), 123–127. https://doi.org/10.1038/sj.jp.7210882

Shelly, G. B., & Vermaat, M. E. (2010). *Discovering computers 2011: Complete.* Cengage Learning.

Slusher, T. M., Olusanya, B. O., Vreman, H. J., Wong, R. J., Brearley, A. M., Vaucher, Y. E., & Stevenson, D. K. (2014). Treatment of neonatal jaundice with filtered sunlight in Nigerian neonates: A randomized controlled trial. *The Lancet Global Health*, 2(10), e596–e605. https://doi.org/10.1016/S2214-109X(14)70305-1

Slusher, T. M., Olusanya, B. O., Vreman, H. J., Wong, R. J., Brearley, A. M., Vaucher, Y. E., & Stevenson, D. K. (2015). A randomized trial of phototherapy with filtered sunlight in African neonates. *New England Journal of Medicine*, 373(12), 1115–1124. https://doi.org/10.1056/NEJ-Moa1501074

Thomke, S. (2003). Experimentation matters: Unlocking the potential of new technologies for innovation. Harvard Business School Press.

Timings, R. L. (2008). *Fabrication and welding engineering*. Newnes.

Valvano, J. W. (2011). *Embedded Microcomputer Systems: Real Time Interfacing* (3rd ed.). Cengage Learning. [Assumed match for Valvano, 2011, as not found in manuscript.]

Vreman, H. J., Wong, R. J., Stevenson, D. K., Route, R. K., Reader, S. D., Fejer, M. M., Gale, R., & Seidman, D. S. (1998). Light-emitting diodes: A novel light source for phototherapy. *Pediatric Research*, 44(5), 804–809. https://doi.org/10.1203/00006450-199811000-00028

Vreman, H. J., Wong, R. J., & Stevenson, D. K. (2004). Phototherapy: Current methods and future directions. *Seminars in Perinatology*, 28(5), 326–333. https://doi.org/10.1053-/j.semperi.2004.09.003

Vreman, H. J., Wong, R. J., Stevenson, D. K., & American Academy of Pediatrics Subcommittee on Hyperbilirubinemia. (2008). Phototherapy for neonatal hyperbilirubinemia: Efficacy, mechanism, and toxicity. *Journal of Perinatology*, 28(Suppl 1), S61–S69. https://doi.org-/10.1038/jp.2008.54

World Health Organization. (2015). *Guidelines on neonatal jaundice*. WHO Press.

Wong, R. J., Vreman, H. J., & Stevenson, D. K. (2002). Quantitation of phototherapy efficacy in neonatal jaundice. *Pediatric Research*, 51(4), 529–533

Yurdakök, M. (2015). Phototherapy in the newborn: What's new? *Journal of Pediatric and Neonatal Individualized Medicine*, 4(2), e040255. https://doi.org/10.7363/040255